THE JOURNAL OF PHYSICAL CHEMISTRY B

ARTICLE

pubs.acs.org/JPCB

Symmetry Breaking and Hydration Structure of Carbonate and Nitrate in Aqueous Solutions: A Study by Ab Initio Quantum Mechanical Charge Field Molecular Dynamics

Viwat Vchirawongkwin,[†] Chinapong Kritayakornupong,[‡] Anan Tongraar,*[,§] and Bernd M. Rode[∥]

[†]Department of Chemistry, Faculty of Science, Chulalongkorn University, Phayathai Road, Patumwan, Bangkok 10330, Thailand

[‡]Department of Chemistry, Faculty of Science, King Mongkut's University of Technology, Thonburi, Bangkok 10140, Thailand

[§]School of Chemistry, Institute of Science, Suranaree University of Technology, Nakhon Ratchasima 30000, Thailand

[∥]Theoretical Chemistry Division, Institute of General, Inorganic and Theoretical Chemistry, University of Innsbruck, Innrain 52a, A-6020 Innsbruck, Austria

ABSTRACT: The ab initio quantum mechanical charge field molecular dynamics (QMCF MD) formalism was applied to simulate carbonate and nitrate anions in aqueous solution. The out-of-plane (ν_2) spectra obtained from the velocity autocorrelation functions (VACFs) and the torsion angle−time functions indicate that the symmetry of carbonate is reduced from D_{3h} to a lower degree by breaking up the molecular plane, whereas the planarity of nitrate anion is retained. The calculated frequencies are in good agreement with the Raman and IR data. Carbonate shows a stronger molecular hydration shell than the nitrate anion with the average molecular coordination numbers of 8.9 and 7.9, respectively. A comparison with the average number of ion−solvent hydrogen bonds (H-bonds) indicates the extra water molecules within the hydration shell of carbonate (∼2) and nitrate (∼3), readily migrating from one coordinating site to another. The mean residence times for water ligands in general classify carbonate and nitrate as moderate and weak structure-making anions, while the specific values for individual sites of nitrate reveal local weak structure-breaking properties.

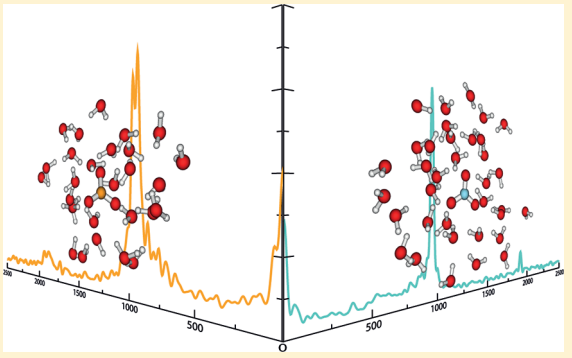

INTRODUCTION

The carbonate and nitrate anions play an important role in biological and environmental systems.[1−3] The level of carbonate anion in seawater relates to atmospheric CO_2.[1] The carbonate is an ubiquitous and reactive anion and reacts to form aqueous and solid state complexes with a majority of metals in the periodic table.[4] The nitrate anion is one of the reactive nitrogen forms, occurring in many biological systems,[3] and a strong oxidizing agent. All nitrate salts are highly soluble. The nitrate anion is also produced in the human body by the oxidation of nitric oxide obtained from the reaction between the enzyme nitric oxide synthase and L-arginine.[5,6] It is interesting that X-ray scattering experiments have investigated many nitrate solutions,[7−11] while experimental data are rare for the carbonate anion. Recent neutron diffraction studies with isotopic substitution were performed for the $CsNO_3$ and Cs_2CO_3 solutions, concluding that hydrogen bonds between water molecules and carbonate are stronger than those formed with nitrate.[12] The reported average coordination number of nitrate is in the range of 5.9 to 9,[13] while it is close to unavailable for carbonate.

The isolated structure of these anions is normally planar with D_{3h} symmetry, which has six normal modes consisting of two single modes, namely, the symmetric stretch (ν_1) and out-of-plane deformation (ν_2), and two doubly degenerate modes, namely, the antisymmetric stretch (ν_3) and in-plane deformation (ν_4). Rudolph et al. reported the symmetry breaking from the D_{3h} to lower symmetry in the concentrated[14] and dilute[15] carbonate solutions due to a strong and asymmetric hydration via Raman and infrared experiments and also optimized the carbonate water cluster with two water molecules employing density functional theory at the B3LYP level with the 6-31+G* basis set in the gas phase, resulting in C_{2v} symmetry.[14] The far-ultraviolet resonance Raman spectroscopy indicates the planarity of nitrate ion in several polar solvents, but with the symmetry being broken from D_{3h} to C_{2v} or C_s due to a very broad band of ν_3.[16,17] The results of photoelectron spectroscopy suggested the first hydration consisting of three water molecules with C_{3h} symmetry for the nitrate ion in aqueous solution.[18] Raman studies have reported that the splitting of ν_3 vanishes for dilute nitrate solutions.[19−21] Recent infrared multiple photon photodissociation experiments of $NO_3^-(H_2O)_n$ clusters, n = 1−6, observed the splitting of ν_3 band due to the perturbation of water molecules, showing the

Received: May 24, 2011
Revised: September 8, 2011
Published: September 20, 2011

dx.doi.org/10.1021/jp204809f | J. Phys. Chem. B 2011, 115, 12527–12536

possible lowering of symmetry to C_1.[22] The weighted average IR spectra of the optimized geometries for the microhydration of carbonate and nitrate anion presented an effect of explicit waters on symmetry lowering.[23,24] The optimization of the carbonate ion in aqueous solution as a dielectric medium employing the electron correlated method with the generalized conductor-like screening model indicated a slight effect of solvent on the geometry compared with the gaseous state.[25] An empirical force field including the out-of-plane displacement of the carbon atom within the carbonate ion was developed to investigate the phase transition of calcite.[26] This potential function was adopted by increasing the stiffness of carbonate ion utilized in the classical molecular dynamics (MD) simulation of calcium carbonate.[27] Recent investigations of the carbonate ion in aqueous solution based on Car−Parrinello (CP) MD simulation discussed the structural properties of the hydration shell without addressing symmetry breaking.[28,29] The inclusion of an intramolecular anharmonic force field in the classical MD simulation[30] and a combined quantum mechanics/molecular mechanics (QM/MM) MD simulation[31] of hydrated nitrate ion presented a splitting of ν_3 in agreement with the spectroscopic results. The reference interaction site model self-consistent field spatial electron density distribution (RISM-SCF-SEDD) provided the evidence of symmetry breaking for the carbonate in the isotropic environment, while the planarity of nitrate anion was claimed.[32] All of these results here motivated us to reinvestigate the influence of hydration on the symmetry breaking and also the characteristics of the hydration structures of both anions by a contemporary ab initio simulation method.

Due to the limitations of conventional QM/MM methods to study composite solutes due to the tedious task to construct intermolecular potential functions accounting for the interactions between each site of solute and water, we applied the ab initio quantum mechanical charge field molecular dynamics (QMCF MD) formalism[33,34] that has already been successfully employed to investigate the structural and dynamical properties of hydrated sulfate,[35,36] phosphate,[37,38] perchlorate,[37,39] bicarbonate,[40,41] and bisulfate[42] anions. The vibrational spectra of the anions in water are evaluated from the velocity autocorrelation functions (VACFs) to investigate the evidence of broken symmetry. The structural properties for each hydration site and the whole molecular shell were obtained via radial distribution functions (RDFs) and coordination number distributions (CNDs). The average number of hydrogen bonds (H-bonds) was also evaluated for each coordinating site to clarify the actual coordination of the solvent. The dynamics were characterized by ligand mean residence times (MRTs). In addition, we evaluated structural and dynamical properties by means of the molecular approach.[40,42]

METHODS

The ab initio QMCF MD formalism has been summarized in detail elsewhere.[33,34] Due to the inclusion of an additional quantum mechanically treated solvent *layer zone* located beyond the first hydration shell of the solute species, the QMCF method avoids the construction of potential functions between the solute and the water molecules; that is, it evades a time-consuming and sometimes hardly tractable task essential in the conventional QM/MM MD formalism.[43−46] The involvement of the point charges of the atoms in the MM region with their changing positions in the core Hamiltonian for the QM calculations is a useful feature of the QMCF MD method with a perturbation term,

$$V' = \sum_{i=1}^{n} \sum_{j=1}^{m} \frac{q_j^{\mathrm{MM}}}{r_{ij}} \tag{1}$$

where n is the number of atoms in the QM region, m is the number of atoms in the MM region, q_j^{MM} is the partial charges of these atoms according to the selected water model, and r_{ij} refers to the distance between a pair of particles in the QM (i) and MM (j) regions. On the other hand, the dynamically changing charges of QM particles, q_i^{QM}, determined by population analysis contribute to the force on each atom j in the MM region as Coulombic forces,

$$F_j^{\mathrm{QM}\rightarrow\mathrm{MM}} = \sum_{i=1}^{n} \frac{q_i^{\mathrm{QM}} \cdot q_j^{\mathrm{MM}}}{r_{ij}} \tag{2}$$

As the conventional QM/MM MD formalism, the QMCF MD method permits the migration of water molecules between the QM and the MM region. For this process, one has to apply a smoothing function,[47]

$$S(r) = \begin{cases} 0 & \text{for } r > r_{\mathrm{on}} \\ \dfrac{(r_{\mathrm{off}}^2 - r^2)^2 (r_{\mathrm{off}}^2 + 2r^2 - 3r_{\mathrm{on}}^2)}{(r_{\mathrm{off}}^2 - r_{\mathrm{on}}^2)^3} & \text{for } r_{\mathrm{on}} \le r \le r_{\mathrm{off}} \\ 1 & \text{for } r < r_{\mathrm{off}} \end{cases} \tag{3}$$

where r is the distance of a given solvent molecule from the center of the simulation box, r_{off} is the radius of the QM region, and r_{on} is the inner border of the smoothing region. The formalism is applied to all atoms of molecules located in the smoothing region, ensuring a continuous transition and change of forces for these molecules according to

$$F_j^{\mathrm{smooth}} = F_j^{\mathrm{MM}} + (F_j^{\mathrm{layer}} - F_j^{\mathrm{MM}}) \times S(r) \tag{4}$$

where F_j^{layer} is the force acting on a particle j located in the (outer QM) smoothing zone and F_j^{MM} is the force acting on a particle j in the MM region. In this context it has to be mentioned that energy is not rigorously conserved, but the related error can be considered very minor due to the short simulation time and the large size of the quantum mechanical region.

The systems consisted of 496 water molecules with one carbonate and one nitrate anion in the carbonate and nitrate solution, respectively. Both solutions were represented by a cubic box of 24.65 Å with periodic boundary conditions. The density of the simulation boxes was 0.997 g cm^{-3}, that is, the experimental value of pure water at 298 K. The simulation was performed in the *NVT* ensemble using a general predictor-corrector algorithm with a time step of 0.2 fs. The system temperature was maintained at 298.16 K by the Berendsen temperature-scaling algorithm[48] with a relaxation time of 100 fs. Although this temperature-scaling algorithm requires, in principle, a long simulation period to sufficiently describe the phase space, a large number of successful publications of QMCF MD simulations[35−42] indicate that our simulation period of 10 ps is adequate to reproduce the properties of hydrated ions well. The QM subregions, namely, the core and layer zone, extended for the carbonate and nitrate anions to 3.5 and 6.0 Å and 3.5 and 6.8 Å, respectively. The structural and dynamical results obtained from our previous

QMCF MD studies[35−42] have also indicated the Hartree−Fock (HF) method to be a good compromise between accuracy and affordable computational effort; thus the quantum mechanical calculation was performed by the HF method with the Dunning double-ζ plus polarization (DZP)[49,50] basis sets for hydrogen and oxygen atoms of water molecules and the Dunning double-ζ plus polarization and diffuse functions (DZP+)[49,50] basis sets for carbon, nitrogen, and oxygen atoms of the carbonate and nitrate anions. Although HF and the methodical problems associated with the thermostat probably leads to slightly underestimated values, our previous study indicated that the associated errors are probably within a 10% to 20% range.[42] The thickness of the smoothing region was chosen as 0.2 Å, corresponding with the smooth exchange of a water between the QM and MM regions of the conventional QM/MM MD formalism.[51] The values of r_{on} and r_{off} are 5.8 and 6.0 Å and 6.6 and 6.8 Å for the carbonate and nitrate anions, according to the RDFs obtained from the equilibrated simulations. The large size of the QM region ensures that it is possible to neglect the interactions between the solute and the solvent molecules in the MM region.[33] The flexible BJH-CF2 water model[52,53] was applied to calculate the interactions between pairs of water in the MM region, with the cutoff distances of 3.0 and 5.0 Å for non-Coulombic interactions between H atoms and between O and H atoms, respectively. According to the verification process by the water simulations in the development of the QMCF MD formalism, this water model satisfied to describe several microscopic and macroscopic properties of water.[33] The partial charges for oxygen and hydrogen atoms in the water molecule according to this model are −0.65966 and +0.32983. This water model supports the fully flexible geometries of water molecules transiting between the QM and MM region. The Coulombic interactions between the Mulliken charges on the atoms within the QM region and the point charges of water molecules according to the BJH-CF2 model are evaluated providing an electrostatic description by a dynamically changing field of point charges, which change according to the movements of atoms inside the QM region and water molecules in the MM region during the simulation. This ensures the continuous adaptation of the Coulombic interactions to all polarization and charge-transfer effects within the solute and surrounding solvent layers.[33,34] In addition, the reaction field method combined with the shifted-force potential technique were applied to account for long-range electrostatic potentials and forces, with a spherical cutoff limit of 12.350 Å. The systems were equilibrated with the QMCF MD method for 50 000 steps (10 ps), and a further 50 000 steps (10 ps) were collected as data sampling for analyzing the structural and dynamical properties. The average number of water molecules in the QM region was 23.6 and 36.6 for the carbonate and nitrate solution, respectively.

The structural and dynamical properties for the hydration shell of carbonate and nitrate anions were evaluated in individual and molecular manners. The molecular hydration shell of these anions was constructed by the combination of all atomic hydration spheres of each anion. The coordinating site for each water molecule to the anions was defined by searching for the shortest distance between the oxygen atom of water molecule and each atom within each anion.[40,42] The molecular RDFs, molecular CNDs, and molecular ligand MRTs for the hydration shell of carbonate and nitrate anions are thus presented in this article. All MRT values were evaluated by the direct method,[54] counting the water exchange processes between hydration shell and bulk. The most appropriate time span to record a water displacement from its original coordination sphere as an exchange process is 0.5 ps,[54,55] which corresponds to the average lifetime of a hydrogen bond in the solvent.[56]

The dynamical properties of a fluid system related to macroscopic transport coefficients can be evaluated from the VACFs, and their Fourier transformations deliver the vibrational spectra via normal-coordinate analysis.[57] The normalized VACF, $C(t)$, is defined as

$$C(t) = \frac{\sum_{i}^{N_t}\sum_{j}^{N} v_j(t_i)v_j(t_i + t)}{N_t N \sum_{i}^{N_t}\sum_{j}^{N} v_j(t_i)v_j(t_i)} \quad (5)$$

where N is the number of particles, N_t is the number of time origins t_i, and v_j denotes a certain velocity component of the particle j. A correlation length of 2.0 ps was used to obtain the power spectra with 4000 averaged time origins.

RESULTS AND DISCUSSION

Structural and Dynamical Properties of CO_3^{2-} and NO_3^- Anions. According to the dynamic movement of all atoms within the systems throughout the simulation period, the averaged geometric parameters such as bond distances, angles, and torsion angles of carbonate and nitrate anions indicate the quality of the selected theoretical level, HF/DZP+, for the QM calculations. The C- and N-torsion angles were defined to investigate the planarity of the solutes as the C−O(1)−O(2)−O(3) and N−O(1)−O(2)−O(3) dihedral angles, respectively. The average C−O distances varying within 0.003 Å are slightly longer than those in the HCO_3^- by 0.04 Å,[40] while the N−O distances varying within 0.002 Å are slightly shorter than those obtained from the conventional HF/MM simulation of nitrate solution by 0.03 Å.[31] These tiny deviations show the similarity of the bonds within each anion. The bond and torsion angles were collected in the form of angular distribution functions (AFDs). The average bond angles around the center atoms again indicate the equivalence of oxygens within each anion. The average C-torsion and N-torsion angles with their deviation of 1° ± 4° and 0° ± 2° reflect the planarity of both anions. Table 1 reports the averaged geometric parameters with their statistical deviation obtained from the QMCF MD simulation, comparing with those parameters obtained from various methods evaluated in the gas phase and solution utilizing the polarizable continuum model (PCM).[58] Our geometry parameters were also compared with those obtained from the reference interaction site model self-consistent field (RISM-SCF) at the HF and B3LYP level with the 6-311+G* basis set.[32] The hybrid B3LYP exchange-correlation functional coupling with the tzvp+ basis set[59] was employed to verify the interpretation of the spectra of photoelectron spectroscopy for the HSO_4^- ion,[60] and this was also applied to verify the theoretical level in our previous work.[42] Thus, we again utilized this basis set coupling with the Hartree−Fock (HF), B3LYP, and quadratic CI calculation including single and double substitutions (QCISD) levels to optimize the geometries of carbonate and nitrate in both phases. The HF/DZP+ level was also employed to investigate the effect of isotropic and uniform field generated by the PCM on the geometries of both anions. The bond distances of anions in the solution phase treated with PCM are shorter than those in gas phase by ca. 0.01 Å, whereas these averaged distances obtained

Table 1. Structural Parameters for the Geometry of CO_3^{2-} and NO_3^- Ions Obtained from Averaging Their Distributions with Their Variations

		HF/DZP+		HF/tzvp+		B3LYP/tzvp+		QCISD/tzvp+		RISM-SCF/6-311+G*[32]	
structural parameter	QMCF MD	gas	PCM	gas	PCM	gas	PCM	gas	PCM	HF	B3LYP
					CO_3^{2-}						
C−O(1) (Å)	1.290 ± 0.035	1.288	1.279	1.286	1.277	1.312	1.302	1.314	1.303	1.267	1.288
C−O(2) (Å)	1.287 ± 0.032	1.288	1.279	1.286	1.277	1.312	1.302	1.314	1.303	1.267	1.288
C−O(3) (Å)	1.290 ± 0.035	1.288	1.279	1.286	1.277	1.312	1.302	1.314	1.303	1.267	1.288
∠O(1)CO(2) (deg)	120 ± 4	120	120	120	120	120	120	120	120	120	120
∠O(2)CO(3) (deg)	120 ± 3	120	120	120	120	120	120	120	120	120	120
C-torsion (deg)	1 ± 4	0	0	0	0	0	0	0	0	7	8
					NO_3^-						
N−O(1) (Å)	1.231 ± 0.023	1.232	1.229	1.231	1.228	1.268	1.265	1.270	1.268	1.217	1.253
N−O(2) (Å)	1.232 ± 0.022	1.232	1.229	1.231	1.228	1.268	1.265	1.270	1.268	1.217	1.253
N−O(3) (Å)	1.233 ± 0.025	1.232	1.229	1.231	1.228	1.268	1.265	1.270	1.268	1.217	1.253
∠O(1)NO(2) (deg)	120 ± 3	120	120	120	120	120	120	120	120	120	120
∠O(2)NO(3) (deg)	120 ± 3	120	120	120	120	120	120	120	120	120	120
N-torsion (deg)	0 ± 2	0	0	0	0	0	0	0	0	0	0

Table 2. C−O and N−O Distances within the $CO_3^{2-}(H_2O)_n$ and $NO_3^-(H_2O)_n$ Clusters Obtained from the Optimizations in the Gas Phase at the HF, MP2, and CCSD Levels

	HF			MP2			CCSD		
n	X−O(1)	X−O(2)	X−O(3)	X−O(1)	X−O(2)	X−O(3)	X−O(1)	X−O(2)	X−O(3)
					CO_3^{2-}				
1	1.292	1.292	1.273	1.325	1.325	1.302	1.319	1.319	1.297
2	1.279	1.296	1.279	1.308	1.330	1.308	1.303	1.324	1.303
3	1.283	1.283	1.283	1.313	1.313	1.313	1.308	1.308	1.308
					NO_3^-				
1	1.235	1.235	1.223	1.282	1.282	1.269	1.274	1.274	1.259
2	1.225	1.239	1.227	1.271	1.290	1.271	1.262	1.282	1.262
3	1.230	1.230	1.230	1.276	1.276	1.276	1.267	1.267	1.267

from the QMCF MD simulations affected by the explicit water molecules are close to those obtained from the HF/DZP+ optimized geometries in the gas phase. To clarify this point, we optimized each anion with one to three water molecules by applying the DZP+ basis set on the atoms within each anion and the DZP basis set on the H and O atoms in water molecules at the HF, MP2, and CCSD levels. The C−O and N−O distances in these small water clusters are listed in Table 2. Their average binding energies are also shown in Table 3. It indicates that the explicit waters with and without the electron correlation effect also affects the bonds in both anions by reducing the distances as in the PCM approach (cf. Table 1). Due to the intermolecular interaction described by the electron correlation method, the MP2 and CCSD levels give stronger binding energies than the HF calculations. With increasing number of water molecules in the system convergence of average binding energies from the HF calculations to the higher methods is observed, especially for the nitrate anion. There is evidence that the perturbation of the Hamiltonian from the point charges in the QMCF MD formalism improves the interactions within the solution, resulting in elongated bond distances that are a good agreement with the

Table 3. Average Binding Energies in kcal mol^{-1} for $CO_3^{2-}(H_2O)_n$ and $NO_3^-(H_2O)_n$ Clusters Obtained from the Optimizations in the Gas Phase at the HF, MP2, and CCSD Levels

n	HF	MP2	CCSD
		CO_3^{2-}	
1	−34.9	−37.3	−36.8
2	−33.4	−35.5	−35.0
3	−32.2	−33.9	−33.4
		NO_3^-	
1	−13.9	−14.1	−14.2
2	−13.3	−13.5	−13.6
3	−12.7	−12.7	−12.8

$C-O_C$ of 1.3 Å and $N-O_N$ in a range from 1.21 ± 0.02 to 1.24 ± 0.02 Å, respectively, reported from the recent neutron diffraction experiments of K_2CO_3[61] and $NaNO_3$[11] solutions.

The C-torsion and N-torsion angles from the gas phase and PCM calculations show the planarity of each anion, but the

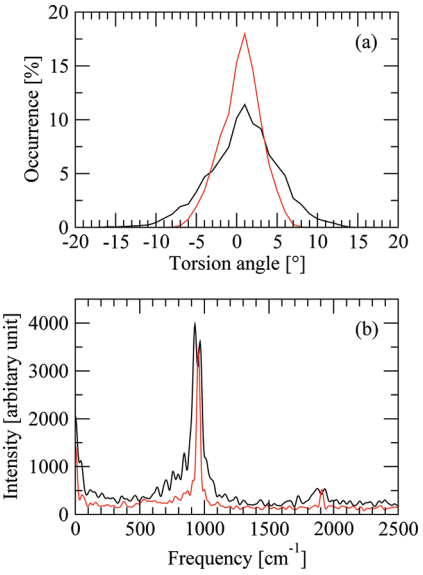

Figure 1. (a) Dihedral angle distribution of the torsion angles and (b) Fourier transformation of the function of time for their angles; the black and red solid lines refer to the C-torsion and N-torsion angles, respectively.

RISM-SCF results indicate a symmetry breaking of the carbonate anion.[32] Although the average C-torsion obtained from the QMCF MD simulations (1° ± 4°) shows a slight removal of the C atom from the molecular plane, it might be a consequence of the limited number of geometries in the short simulation period of 10 ps. It is interesting to investigate the possibility of the symmetry breaking for both anions. According to the motion of all atoms in the MD formalism, the center atoms also oscillate during the simulation period. The ADFs in Figure 1a present a higher flexibility of C-torsion (−14° to 16°) compared to the N-torsion (−8° to 8°). The Fourier transformations for the C-torsion and N-torsion as the function of time are shown in Figure 1b, presenting two peaks situated at 927 and 967 cm^{-1} for the carbonate, and the peak at 953 cm^{-1} for the nitrate anion. These values correspond to the out-of-plane deformation (ν_2) reported from Raman experiments at 884 and 832 cm^{-1} for the carbonate and nitrate anions.[14] The spectra in Figure 1b also display small peaks with a low intensity at 1873 and 1930 cm^{-1} for the carbonate and at 1910 cm^{-1} for the nitrate anion, corresponding to the Raman observations for the overtone of the out-of-plane deformation ($2\nu_2$) at 1764 and 1658 cm^{-1} in carbonate[14,15] and nitrate[16,17,21] solutions, respectively. The differences of ν_2 frequencies between both anions and between the atomic masses of C and N are small; thus the harmonic motion and its force constant of C-torsion and N-torsion should be similar. Whereas a significant difference of both anions is observed, the range of C-torsion in Figure 1a is ca. two times that of the N-torsion ADF. The agreements of QM calculations, RISM-SCFs, and our QMCF MD simulation let us conclude that the nitrate anion mostly retains its planarity in the solution. The symmetric band of the N−torsion corresponds to an out-of-plane displacement of N atom around 0°, implying the amplitude of this oscillation in the QMCF MD simulation be 8°. The range of the C-torsion covers the value of ±7° reported from the RISM-SCF/HF[32] and an oscillating amplitude of ±8°, indicating the occurrence of symmetry breaking for the carbonate anion in solution during the simulation period.

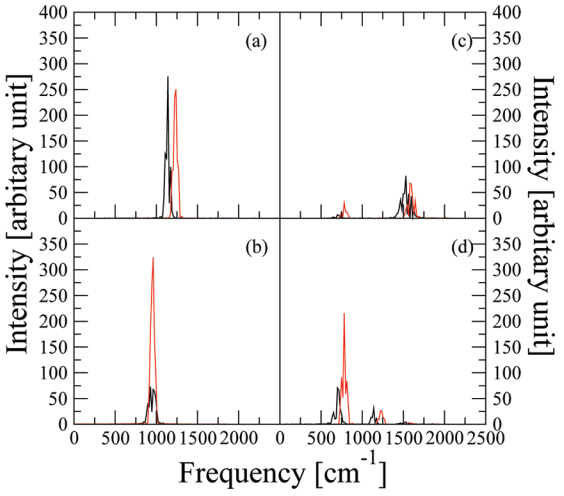

Figure 2. Power spectra of (a) ν_1, (b) ν_2, (c) ν_3, and (d) ν_4 modes for the D_{3h} symmetry of CO_3^{2-} (black solid lines) and NO_3^- (red solid lines) anions.

One dynamical property, namely, the vibrational spectrum, is an important property as it can be compared with the Raman (R) and infrared (IR) data. The spectra calculated via VACFs from the QMCF MD simulation require an assignment of the point group to the solute. The nitrate anion has approximately identical bond distances and planar geometry of D_{3h} symmetry. Although there is evidence indicating symmetry breaking for the carbonate anion, we also assumed a molecular plane with the D_{3h} symmetry for this anion due to a low barrier of the free energy surface (less than 5 kcal mol^{-1}) obtained from the RISM-SCF calculations[32] and a symmetric oscillation of the C atom throughout the simulation period. Four fundamental modes of the D_{3h} symmetry will span the following representation:

$$\Gamma(D_{3h}) = a_1'(\mathrm{R}) + 2e'(\mathrm{R,IR}) + a''_2(\mathrm{IR}) \quad (6)$$

These modes consist of the symmetric stretch, $\nu_1(a'_1)$, the out-of-plane deformation, $\nu_2(a''_2)$, the antisymmetric stretch, $\nu_3(e')$, and the in-plane deformation, $\nu_4(e')$ modes. The power spectra of these normal modes for the carbonate and nitrate anions predicted by the QMCF MD simulations are displayed in Figure 2, and the frequencies of peaks for each mode are listed in Table 4.

The bands of ν_2 in Figure 2b, showing a split peak for the carbonate anion, have a similar pattern with the Fourier transformations for the C-torsion and N-torsion as the function of time in Figure 1b; however, the overtone peaks disappear in the spectra obtained from the VACFs. This again confirms the broken symmetry of the carbonate anion's molecular plane, while the plane is still retained in the nitrate anion. The ν_3 and ν_4 are degenerate modes, presented by the dominant band with the appearance of a minor band of another mode in the spectrum of each mode. Furthermore, ν_4 also appears as a minor peak of ν_1, according to a contamination of bond stretching in a vector projection. The calculated ν_3 and ν_4 spectra with a band characteristic interpreted as a reduction of symmetry to C_{2v} or to C_s[16,17] correspond to the dynamical motions of these anions within the environment of explicit waters during the simulation period. The frequencies of the solutes within the optimized $CO_3^{2-}(H_2O)_3$ and $NO_3^-(H_2O)_3$ clusters evaluated at the MP2 and CCSD levels are also listed in Table 4. MP2 and CCSD

predict a lower ν_1 of the carbonate anion than the experimental value, reflecting an overestimated interaction of the solute with water molecules. However, these correlated methods indicate a weak interaction of nitrate anion with solvent resulting in a higher ν_1 than the Raman result. To further investigate the influence of correlation in the liquid state was impossible, as the application of these methods in the QMCF simulations is beyond present computational feasibility. All calculated frequencies obtained without applying a scaling factor from the QMCF MD simulations are higher than the values reported from the Raman experiment[14] by ~230 cm^{-1}. We also calculated the frequencies scaled with the factor 0.902 obtained from the correction of the QMCF MD results with the coupled-cluster singles and doubles (CCSD) level.[36] The scaled frequencies of carbonate anion are red-shifted by ~50 cm^{-1}, while the scaled ν_1, ν_2, and ν_3 of the nitrate anion are blue-shifted by ~80 cm^{-1} compared with the experimental data.[14] The agreement of calculated frequencies, especially the scaled values, for these modes with the experimental data again shows the reliability of the QMCF MD simulation to acquire dynamical properties of the solutes.[37−42]

Table 4. Vibration Frequencies (cm^{-1}) for Each Normal Mode of CO_3^{2-} and NO_3^- Anions Evaluated by the VACFs of QMCF MD Simulations, Given Scaled by the Factor 0.902[36] in Parentheses

	frequency (cm^{-1})			
	$\nu_1(a'_1)$	$\nu_2(a''_2)$	$\nu_3(e')$	$\nu_4(e')$
		CO_3^{2-}		
QMCF MD	1140 (1028)	928, 961 (837, 867)	1531 (1381)	700 (631)
MP2	1026	841	1403	684
CCSD	1046	864	1432	692
exptl[14]	1066	884	1385	684
		NO_3^-		
QMCF MD	1238 (1117)	961 (867)	1580 (1425)	782 (705)
MP2	1070	790	1529	712
CCSD	1088	821	1440	715
HF/MM MD[a,31]	1088	712	1401, 1441	709
B3LYP/MM MD[b,31]	965	710	1237, 1313	649
exptl[14]	1048	832	1348	718

[a] The reported values are scaled by 0.9051. [b] The reported values are scaled by 0.9614.

Structural and Dynamical Properties of the Hydration Shell. According to the preliminary equilibrations of system boxes, their RDFs, or $g_{\alpha\beta}(r)$, suggested that the boundary of QM region should be selected as 6.0 and 6.8 Å for the carbonate and nitrate solutions. The larger QM size for the nitrate system is caused by the weak interactions between the anion with its hydration shell, resulting in a larger number of water molecules within this region during the simulation period than in the case of carbonate anion (ca. 13 molecules). The boundary of the hydration shell from the C···O_{water} and N···O_{water} RDFs is located at 4.48 Å and 4.74 Å, respectively, which implies that the hydration shell of the center atom extends from the terminal oxygens to 3.19 and 3.51 Å for the carbonate and nitrate anion. The O(1), O(2), and O(3) atoms were assigned to represent the coordinating sites for both anions producing the hydration shell around each molecular solute. The individual RDF of each site associated with its CND for both anions are displayed in Figure 3. The height of $g_{\alpha\beta}(r_{max})$ for the carbonate indicates a stronger structure of the individual hydration shells than those of the nitrate anion, agreeing with the results that the water molecules form stronger hydrogen bonds with carbonate than nitrate anion concluded from the neutron diffraction with isotopic substitution (NDIS) of Cs_2CO_3 and $CsNO_3$ in aqueous solutions.[12] It is in good agreement with average binding energies of the small water clusters for the carbonate and nitrate anions calculated at the various levels shown in Table 3, which also indicates the stronger hydration shell of carbonate than that of nitrate anion. The first peak of (site)···O_{water} RDFs for the carbonate anion situated at 2.70 Å is in good agreement with those obtained from the first classical MD for this anion (2.69 Å),[27] while the slightly shorter (~0.06 Å) peak of (site)···H_{water} RDFs from the QMCF MD simulation than those from the classical MD (1.78 Å)[27] reflects a stronger hydrogen bonding caused by quantum effects. For the nitrate anion, the first peak of (site)···O_{water} RDFs from the QMCF MD simulation is slightly longer than those obtained

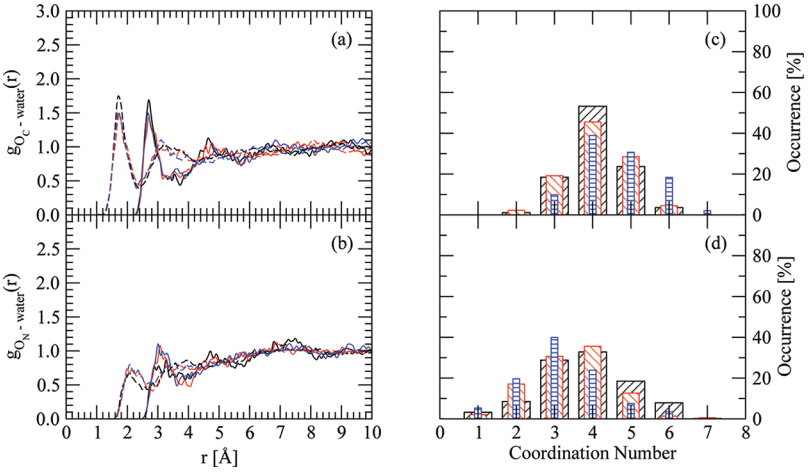

Figure 3. Individual RDF plots of (a) O_C—water and (b) O_N—water, which solid and dashed lines refer to the RDFs for the O and H atoms of water, for CO_3^{2-} and NO_3^- anions, respectively. Hydration shell CNDs of each O sites within the (c) CO_3^{2-} and (d) NO_3^- anions. The black, red, and blue colors refer to the O(1), O(2), and O(3) atoms within each anion, respectively.

Table 5. Characteristic Values of the Radial Distribution Function $g_{\alpha\beta}(r)$ for Each Site of CO_3^{2-} and NO_3^- Anions in the Hydration Shell Determined by the QMCF MD Simulation

coordinating site	$r_{max}(O_w)^a$	$r_{min}(O_w)^a$	$r_{max}(H_w)^a$	$r_{min}(H_w)^a$	n^a
		CO_3^{2-}			
O(1)	2.70	3.72	1.71	2.38	4.1
O(2)	2.70	3.74	1.74	2.40	4.1
O(3)	2.68	3.87	1.72	2.30	4.6
surface	2.70	3.82	1.72	2.44	8.9
		NO_3^-			
O(1)	3.28	3.90	2.07	2.66	3.8
O(2)	3.08	3.76	1.99	2.82	3.4
O(3)	3.00	3.62	2.08	2.86	3.2
surface	3.02	3.72	2.08	2.88	7.9

[a] r_{max} and r_{min} are the distances of the maximum and minimum of $g_{\alpha\beta}(r)$ for the hydration shell in Å, and n is the averaged coordination numbers of the shell, respectively.

from the recent classical MD simulated $NaNO_3$ solution (2.83 Å).[11] However, our results are in good agreement with the distances obtained from the X-ray scattering measurements of 2.88, 2.87−2.95, 2.86−3.00, and 2.90−2.95 for the NH_4NO_3,[7] $NaNO_3$,[8] $AgNO_3$,[9] and $Rh(NO_3)_3$[10] solutions, respectively. This again indicates the reliability of individual hydration structures for both anions obtained from the QMCF MD simulations. The individual CNDs were evaluated based on the minimum of RDFs for each site and are listed in Table 5. The range of averaged coordination numbers (CNs) from 4.1 to 4.6 for the carbonate also proves stronger interactions of each site with its hydration shell than those of nitrate anion with the range of 3.2−3.8. The observed small deviations of individual CNs are considered as insignificant due to the short sampling time, which would not cover all possible configurations. However, the individual CNs of water molecules coordinating with each oxygen of nitrate anion obtained from the QMCF MD simulation are larger than the values of 1−2 molecules expected from the averaged CN of 5.9−9 from the X-ray scattering results.[13] For the carbonate anion, no such experimental data have been reported yet.

According to the overlapping of all individual hydration spheres in the anions, the direct sum of these CNs is unable to refer to the molecular CN of solutes.[62] We thus evaluated the molecular RDFs and CNDs for both anions, utilizing the radius of hydration spheres for each (site)···O_{water} RDF as the criterion to assign the coordinating site for each water molecule[35,40,42] shown in Figure 4. The density of water molecules presented in the molecular RDFs was evaluated in the domain produced by the union of spheres having the same radii, by assigning the coordination site with the shortest distance among the values obtained from the oxygen of water and each site within the solute. The molecular CNDs were evaluated on the molecular domain, constructed by applying the boundary obtained from the individual RDF for each site of the solute.[62] The characteristic values of molecular hydration shells and their averaged CNs from the molecular surface−water RDFs and CNDs are also listed in Table 5. The height of molecular RDFs indicates that the molecular hydrations of both anions is well-defined with a more pronounced structure than in the separate investigations of each hydration site. The higher CNs of carbonate (12.8) and nitrate (10.4) anions from the direct sum of individual CNs than in the corresponding molecular CN, differing by 3.9 and 2.5 molecules, indicate the location of waters in the intersection of the individual hydration spheres, causing on overcounting of CN as observed also in the hydration structures of sulfate,[35] bicarbonate,[40] and bisulfate[42] anions. These results support the possibility that the water molecules within the molecular hydration shell are able to rapidly change the coordinating site around the solute during the simulation period. The molecular CN of 7.9 for the nitrate anion is in excellent agreement with the accepted experimental data (5.9−9),[13] and hence the molecular CN of 8.9 produced for carbonate anion appears reliable as well.

Table 6. Average Number of Hydrogen Bonds for Each O Site and Molecular Surface of CO_3^{2-} and NO_3^- Anions in the Simulation Period

	O(1)	O(2)	O(3)	surface
CO_3^{2-}	2.5 ± 0.6	2.3 ± 0.7	2.2 ± 0.7	7.0 ± 1.1
NO_3^-	1.6 ± 0.9	1.8 ± 0.9	1.8 ± 1.0	5.2 ± 1.4

To clarify the dynamical change of the water molecules between coordination sites, the number of H-bonds can be taken as a measure for the actual contacts between solute and hydrating water molecules, also indicating possible migrations of available extra molecules to other sites.[42] Since the definition of H-bond has been expressed by two different ways, namely, by energetic and geometric criteria,[63,64] we utilized the structural criterion depending on the cutoff parameters (distances $R_{HO}^{(c)}$ and $R_{OO}^{(c)}$, and angle $\phi^{(c)}$) in analogy to water-dimethyl sulfoxide mixtures[65] and our previous studies.[41,42] The cutoff distances $R_{HO}^{(c)}$ and $R_{OO}^{(c)}$ for each oxygen site were obtained from the corresponding ((site)···H_{water} and (site)···O_{water}) RDFs. The angle $\phi^{(c)}$ was set to 30°.[65] The average numbers of H-bonds for the carbonate and nitrate anions are listed in Table 6. The average H-bond numbers for the molecular hydration (or the surface) was calculated by averaging the summation of all H-bonds in each time step over the simulation period. The equivalence between the direct sum of each site and the surface values shows the formation of H-bond between the water molecule and the coordinating site ratio as 1:1, resulting in the actual CN for the carbonate (7.0) and nitrate (5.2) anions. These H-bond data compared with the molecular CNs (8.9 and 7.9 for the carbonate and nitrate anion, respectively) also point at some extra water molecules located in the molecular hydration shell of carbonate (∼2) and nitrate (∼3) anions without forming H-bonds to the solutes, readily changing the coordinating site, and representing a weaker hydration. The smaller number of extra waters for carbonate compared to nitrate also indicates a stronger hydration structure of the former than the latter anion. It is obvious that the molecular charge also affects the number of H-bonds formed to each oxygen site, resulting in this stronger hydration structure of carbonate compared to nitrate (also see Figure 4) as concluded also from the NDIS experiment.[12]

The dynamics of water molecules within the hydration shell of both anions were analyzed by the ligand MRT evaluated by the direct method,[54] dividing the average number of water molecules within the hydration shell throughout the simulation time by the number of exchange events with two time parameters, $t^* = 0.0$ and 0.5 ps, corresponding to all displacements and to sustainable exchange events.[56] MRT values for all coordinating sites of both anions are listed in Table 7, compared with the data of pure water

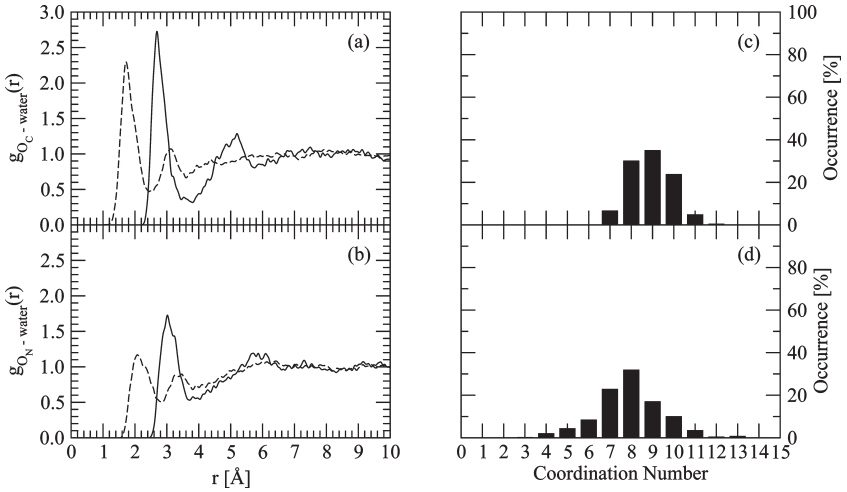

Figure 4. Molecular RDF plots of (a) CO_3^{2-} and NO_3^- anions obtained from the QMCF MD simulation evaluated by means of the combination of spheres; solid and dashed lines refer to the RDFs for the O and H atoms of water, respectively. The molecular hydration shell CND of (c) CO_3^{2-} and (d) NO_3^- anions is shown.

Table 7. Mean Ligand Residence Time τ (ps), Number of Accounted Ligand Exchange Events N, and Total Number of Processes Needed for One Successful Water Exchange R_{ex} Obtained from the QMCF MD Simulations

	t^* = 0.0 ps			t^* = 0.5 ps			
	N_{inv} [a]	$N_{ex}^{0.0}$/10 ps [b]	$\tau_D^{0.0c}$	N_{inv} [a]	$N_{ex}^{0.5}$/10 ps [b]	$\tau_D^{0.5c}$	R_{ex} [d]
				CO_3^{2-}			
O(1)	29	170	0.25	16	27	1.56	6.3
O(2)	30	195	0.22	17	27	1.58	7.2
O(3)	32	222	0.22	14	23	2.08	9.6
surface	40	171	0.53	26	39	2.31	4.4
				NO_3^-			
O(1)	30	206	0.19	14	37	1.04	5.6
O(2)	27	155	0.23	15	36	0.98	4.3
O(3)	27	176	0.18	12	33	0.99	5.3
surface	35	245	0.32	22	44	1.81	5.6
H_2O [e]		269[54]	0.2,[54] 0.33[55]		24[54]	1.7,[54] 1.51[55]	11.2[54]
H_2O		131[f]	0.2[f], 0.55[56]		20[f]	1.3[f]	6.5[f]

[a] Number of ligands involved in the MRT evaluation according to the value of t^*. [b] Number of accounted exchange events per 10 ps lasting at least 0.0 and 0.5 ps, respectively. [c] Mean residence time determined by the direct method[54] in picoseconds. [d] Average number of processes needed for one successful ligand exchange. [e] Values obtained from a QM/MM-MD simulation of pure water [54,55] in picoseconds. [f] Unpublished results: values obtained from a QMCF MD simulation of pure water in picoseconds.

simulations.[54,55] The number of involved ligands (N_{inv}) represents the coordination of water molecules with the evaluated site in the criterion of t^*, while the number of accounted exchange events (N_{ex}) accumulates the exchange processes of N_{inv} throughout the simulation period. The carbonate has a greater total number of individual and molecular N_{inv} than the nitrate anion, corresponding to the stronger hydration structure and larger CNs of the former as discussed from the RDFs and CNDs. The greater value of the total individual N_{inv} than the molecular N_{inv} includes the movements of waters among the coordinating sites in the molecular hydration shell. The difference value between the total $N_{ex}^{0.5}$ and the molecular $N_{ex}^{0.5}$ implies that the migrations of water molecules between the coordinating sites were 38 and 62 processes (approximately half of the exchange events) for carbonate and nitrate, respectively, similar as for the HCO_3^-[40] and HSO_4^-[42] anions. The lower molecular N_{ex} of carbonate again indicates the stronger hydration shell than that of nitrate. The standard relaxation time used in the direct method with t^* = 0.5 ps leads to the MRT of water ligands at the coordinating sites, while the hydrogen bond lifetimes can be estimated with t^* = 0.0 ps.[40,54] Our MRT results compared with the simulations of pure water[54,55] classify carbonate as a structure-making anion, while the nitrate anion presents a more complicated situation. The individual MRTs of nitrate anion present a higher mobility of water molecules than those in pure water as reported in the previous conventional QM/MM MD study,[31] while the molecular data indicate a stronger hydration structure. Thus, we can classify the nitrate anion as a weak structure-maker as a whole, but with local structure-breaking ability near the coordination sites. The number of processes needed for one successful water exchange, R_{ex}, being the ratio of $N_{ex}^{0.0}$ to $N_{ex}^{0.5}$ for the carbonate anion also shows such peculiar processes, according to the significant difference between the individual and molecular R_{ex}. The R_{ex} for the interchanging of coordinating site within the molecular hydration shell was 10.9 and 4.7 for carbonate and nitrate, respectively, reflecting the ease of migration for the water ligands within the hydration shell of the latter.

CONCLUSION

The aqueous solutions of carbonate and nitrate anion were simulated with the QMCF MD methodology to obtain structural and dynamical properties not only of their hydration shells, but also of the anions themselves. Our results give sufficient evidence of symmetry breaking from D_{3h} to a lower degree, while the nitrate anion seems to retain its planar structure. These results are also supported by the RISM-SCF-SEDD data.[32] The vibrational spectra obtained from the VACFs are in good agreement with the experimental observations,[14−17,21] again indicating the validity of vector projections in the normal mode analysis. We also presented the correlation between the power spectrum of

the torsion angle−time functions and the out-of-plane (ν_2) mode, showing a new possibility to obtain the vibration spectrum without the evaluation of VACFs. A good agreement of (site)···O_{water} RDFs was achieved with the X-ray scattering data for nitrate,[7−10] indicating the accuracy of QMCF MD simulations to acquire the hydration structure of solutes as in previous studies.[35,37−40,42] Although such experimental data for the carbonate anion are missing to be compared with our results, the hydration structure of this anion is also assumed as reliable. The molecular approach[40,42] was applied to investigate the structural and dynamical properties for both anions. It indicates the location of water molecules within the intersection volumes of individual hydration spheres of both anions. The number of H-bonds shows the molecular hydration shell of anions consisting of the actual bound and extra water molecules readily migrating from one coordinating site to be other. The smaller number of such extra water for carbonate (∼2) than for nitrate (∼3) reflects the stronger hydration structure of the former, which is also confirmed by the MRTs for individual sites and the molecule as a whole. While carbonate is a structure-making anion, the individual MRTs of nitrate anion present a structure-breaking property, while the molecular value lets it appears as a weak structure-maker.

AUTHOR INFORMATION

Corresponding Author
*E-mail: anan_tongraar@yahoo.com.

ACKNOWLEDGMENT

Generous financial support by the Austrian Science Foundation (FWF) and ASEA-UNINET, the National Research University (NRU) Project of Thailand's Office of the Higher Education Commission, and Centre for Petroleum, Petrochemicals and Advanced Materials, Chulalongkorn University are gratefully acknowledged. A.T. acknowledges support by the Thailand Research Fund (TRF) and Suranaree University of Technology (SUT). This work is also financial supported by the National Research Council of Thailand (NRCT) and the commission of Higher Education (CHE).

REFERENCES

(1) Elderfield, H. *Science* **2002**, *296*, 1618–1621.
(2) Bloom, A. J.; Burger, M.; Asensio, J. S. R.; Cousins, A. B. *Science* **2010**, *328*, 899–903.
(3) Sutton, M. A.; Oenema, O.; Erisman, J. W.; Leip, A.; van Grinsven, H.; Winiwarter, W. *Nature* **2011**, *427*, 159–161.
(4) Bargar, J. R.; Kubicki, J. D.; Reitmeyer, R.; Davis, J. A. *Geochim. Cosmochim. Acta* **2005**, *69*, 1527–1542.
(5) Mitchell, H. H.; Shonle, H. A.; Grindley, H. S. *J. Biol. Chem.* **1916**, *24*, 461–490.
(6) Benjamin, N. *Ann. Zootech.* **2000**, *49*, 207–216.
(7) Caminiti, R.; Licheri, G.; Piccaluga, G.; Pinna, G. *J. Chem. Phys.* **1978**, *68*, 1967–1970.
(8) Caminiti, R.; Licheri, G.; Paschina, G.; Piccaluga, G.; Pinna, G. *J. Chem. Phys.* **1980**, *72*, 4522–4528.
(9) Yamaguchi, T.; Johansson, G.; Holmberg, B.; Maeda, M.; Ohtaki, H. *Acta Chem. Scand.* **1984**, *A38*, 437–451.
(10) Caminiti, R.; Atzei, D.; Cucca, P.; Anedda, A.; Bongiovanni, G. *J. Phys. Chem.* **1986**, *90*, 238–243.
(11) Megyes, T.; Bálint, S.; Peter, E.; Grósz, T.; Bakó, I.; Krienke, H.; Bellissent-Funel, M.-C. *J. Phys. Chem. B* **2009**, *113*, 4054–4064.
(12) Mason, P. E.; Neilson, G. W.; Dempsey, C. E.; Brady, J. W. *J. Am. Chem. Soc.* **2006**, *128*, 15136–15144.
(13) Ohtaki, H.; Radnai, T. *Chem. Rev.* **1993**, *93*, 1157–1204.
(14) Rudolph, W. W.; Fischer, D.; Irmer, G. *Appl. Spectrosc.* **2006**, *60*, 130–144.
(15) Rudolph, W. W.; Irmer, G.; Königsberger, E. *Dalton Trans.* **2008**, 900–908.
(16) Waterland, M. R.; Kelley, A. M. *J. Chem. Phys.* **2000**, *113*, 6760–6773.
(17) Waterland, M. R.; Stockwell, D.; Kelley, A. M. *J. Chem. Phys.* **2001**, *114*, 6249–6258.
(18) Wang, X.-B.; Yang, X.; Wang, L.-S.; Nicholas, J. B. *J. Chem. Phys.* **2002**, *116*, 561–570.
(19) Chang, T. G.; Irish, D. E. *J. Phys. Chem.* **1973**, *77*, 52–57.
(20) Zhang, Y.-H.; Choi, M. Y.; Chan, C. K. *J. Phys. Chem. A* **2004**, *108*, 1712–1718.
(21) Wahab, A.; Mahiuddin, S.; Hefter, G.; Kunz, W.; Minofar, B.; Jungwirth, P. *J. Phys. Chem. B* **2005**, *109*, 24108–24120.
(22) Goebbert, D. J.; Garand, E.; Wende, T.; Bergmann, R.; Meijer, G.; Asmis, K. R.; Neumark, D. M. *J. Phys. Chem. A* **2009**, *113*, 7584–7592.
(23) Pathak, A. K.; Mukherjee, T.; Maity, D. K. *J. Phys. Chem. A* **2008**, *112*, 3399–3408.
(24) Pathak, A. K.; Maity, D. K. *J. Phys. Chem. A* **2009**, *113*, 13443–13447.
(25) Stefanovich, E. V.; Boldyrev, A. I.; Truong, T. N.; Simons, J. *J. Phys. Chem. B* **1998**, *102*, 4205–4208.
(26) Archer, T. D.; Birse, S. E. A.; Dove, M. T.; Redfern, S. A. T.; Gale, J. D.; Cygan, R. T. *Phys. Chem. Miner.* **2003**, *30*, 416–424.
(27) Bruneval, F.; Donadio, D.; Parrinello, M. *J. Phys. Chem. B* **2007**, *111*, 12219–12227.
(28) Tommaso, D. D.; de Leeuw, N. H. *J. Phys. Chem. B* **2008**, *112*, 6965–6975.
(29) Kumar, P. P.; Kalinichev, A. G.; Kirkpatrick, R. J. *J. Phys. Chem. B* **2009**, *113*, 794–802.
(30) Ebner, C.; Sansone, R.; Hengrasmee, S.; Probst, M. *Int. J. Quantum Chem.* **1999**, *75*, 805–814.
(31) Tongraar, A.; Tangkawanwanit, P.; Rode, B. M. *J. Phys. Chem. A* **2006**, *110*, 12918–12926.
(32) Vchirawongkwin, V.; Sato, H.; Sakaki, S. *J. Phys. Chem. B* **2010**, *114*, 10513–10519.
(33) Rode, B. M.; Hofer, T. S.; Randolf, B. R.; Schwenk, C. F.; Xenides, D.; Vchirawongkwin, V. *Theor. Chem. Acc.* **2006**, *115*, 77–85.
(34) Hofer, T. S.; Pribil, A. B.; Randolf, B. R.; Rode, B. M. Ab Initio Quantum Mechanical Charge Field Molecular Dynamics: A Nonparametrized First-Principle Approach to Liquids and Solutions. In *Combining Quantum Mechanics and Molecular Mechanics. Some Recent Progresses in QM/MM Methods*; Sabin, J. R., Brändas, E., Eds.; Academic Press: New York, 2010; Vol. 59, pp 213−246.
(35) Vchirawongkwin, V.; Rode, B. M.; Persson, I. *J. Phys. Chem. B* **2007**, *111*, 4150–4155.
(36) Vchirawongkwin, V.; Rode, B. M. *Chem. Phys. Lett.* **2007**, *443*, 4152–157.
(37) Pribil, A. B.; Vchirawongkwin, V.; Hofer, T. S.; Randolf, B. R. Structure and Dynamics of Composite Anions in Aqueous Solution. *Computation in Modern Science and Engineering, Proceedings of the International Conference on Computational Methods in Science and Engineering*, 2007; pp 921−923.
(38) Pribil, A. B.; Hofer, T. S.; Randolf, B. R.; Rode, B. M. *J. Comput. Chem.* **2008**, *29*, 2330–2334.
(39) Pribil, A. B.; Hofer, T. S.; Vchirawongkwin, V.; Randolf, B. R.; Rode, B. M. *Chem. Phys.* **2008**, *346*, 182–185.
(40) Vchirawongkwin, V.; Pribil, A. B.; Rode, B. M. *J. Comput. Chem.* **2010**, *31*, 249–257.
(41) Vchirawongkwin, V.; Kritayakornupong, C.; Ruangpornvisuti, V.; Rode, B. M. *J. Mol. Struct.: THEOCHEM* **2009**, *913*, 236–239.
(42) Vchirawongkwin, V.; Kritayakornupong, C.; Rode, B. M. *J. Phys. Chem. B* **2010**, *114*, 11561–11569.
(43) Warshel, A.; Levitt, M. *J. Mol. Biol.* **1976**, *103*, 227–249.
(44) Field, M. J.; Bash, P. A.; Karplus, M. *J. Comput. Chem.* **1990**, *11*, 700–733.

(45) Gao, J. *J. Am. Chem. Soc.* **1993**, *115*, 2930–2935.
(46) Bakowise, D.; Thiel, W. *J. Phys. Chem.* **1996**, *100*, 10580–10594.
(47) Brooks, B. R.; Bruccoleri, R. E.; Olafson, B. D.; States, B. D.; Swaminathan, S.; Karplus, M. *J. Comput. Chem.* **1983**, *4*, 187–217.
(48) Berendsen, H. J. C.; Postma, J. P. M.; van Gunsteren, W. F.; DiNola, A.; Haak, J. R. *J. Chem. Phys.* **1984**, *81*, 3684–3690.
(49) Dunning, T. H., Jr.; Hay, P. J. In *Gaussian Basis Sets for Molecular Calculations*; Schaefer, H. F., III, Ed.; Plenum Press: New York, 1977; Vol. 3, Chapter 1, pp 1−27.
(50) Dunning, T. H., Jr. *J. Chem. Phys.* **1970**, *53*, 2823–2833.
(51) Tongraar, A.; Sagarik, K.; Rode, B. M. *Phys. Chem. Chem. Phys.* **2002**, *4*, 628–634.
(52) Stillinger, F. H.; Rahman, A. *J. Chem. Phys.* **1978**, *68*, 666–670.
(53) Bopp, P.; Janscó, G.; Heinzinger, K. *Chem. Phys. Lett.* **1983**, *98*, 129–133.
(54) Hofer, T. S.; Tran, H. T.; Schwenk, C. F.; Rode, B. M. *J. Comput. Chem.* **2004**, *25*, 211–217.
(55) Xenides, D.; Randolf, B. R.; Rode, B. M. *J. Chem. Phys.* **2005**, *122*, 174506.
(56) Lock, A. J.; Woutersen, S.; Bakker, H. J. *J. Phys. Chem. A* **2001**, *105*, 1238–1243.
(57) Bopp, P. *Chem. Phys.* **1986**, *106*, 205–212.
(58) Frisch, M. J. et al. *Gaussian 03*, Revision D.02; Gaussian, Inc.: Wallingford, CT, 2004.
(59) Godbout, N.; Salahub, D. R.; Andzelm, J.; Wimmer, E. *Can. J. Chem.* **1992**, *70*, 560–571.
(60) Wang, X.-B.; Nicholas, J. B.; Wang, L.-S. *J. Phys. Chem. A* **2000**, *104*, 504–508.
(61) Kameda, Y.; Sasaki, M.; Hino, S.; Amo, Y.; Usuki, T. *Phys. B: Condens. Matter* **2006**, *385*−*386*, 279–281; Proceedings of the Eighth International Conference on Neutron Scattering.
(62) Vchirawongkwin, S.; Vchirawongkwin, V. *Comput. Theoret. Chem.* **2011**, *974*, 26–30.
(63) Sceats, M. G.; Rice, S. A. *J. Chem. Phys.* **1980**, *72*, 3236–3247.
(64) Mezei, M.; Beveridge, D. L. *J. Chem. Phys.* **1981**, *74*, 622–632.
(65) Luzar, A.; Chandler, D. *J. Chem. Phys.* **1993**, *98*, 8160–8173.